Supporting Information

Li *et al*. Genomic and environmental determinants and their interplay underlying phenotypic plasticity

SI Materials and Methods

Population and phenotyping. The population was evaluated at seven environments: Guayanilla, Puerto Rico (winter nursery in 2010-11 and 2011-12: PR11 and PR12, and summer nursery 2014: PR14S); Manhattan, KS (summer nursery in 2011 and 2012: KS11 and KS12); and Ames, IA (summer nursery in 2013 and 2014: IA13 and IA14) (table S1, dataset S1).

In sorghum, G × E in flowering time can be due to differing responses to temperature and photoperiod (1). Puerto Rico is a tropical island with day length ranges from below 12 to higher than 14 hours and an average temperature of 82.4 °F (28.0 °C) throughout the year. The conditions in Puerto Rico during winter seasons are similar to the climate of northeastern Africa, where sorghum originated. The day length is less than 12 hours, an inductive condition for sorghum to flower. Summer seasons in Kansas are long day with high temperature around 90 °F (32.2 °C). The day length is more than 14 hours which can suppress flowering. The day length in Iowa is the longest of the three geographical locations. However, the temperature from June to August is around 70 °F (21.1 °C).

Environment analysis and search for an environmental index. Clustering analysis of seven environments was carried out based on 1) photoperiod, 2) daily unit of growing degree days (GDD) from 1 day after planting (DAP) to 120 DAP, and 3) observed flowering time of the population. Hierarchical clustering with Euclidean distance and the Ward's method was used in clustering analysis. In addition, the RILs were clustered using hierarchical clustering, and principal component analysis was carried out with the flowering time data collected in seven environments.

The high correlation between photothermal time (PTT) measurements and population means across environments can be interpreted as follows. At each environment, the population mean of flowering time expressed as GDD was obtained by averaging across 237 RILs. With such a large sample size, the final phenotype (population mean) is an accurate reflection of that environment on the whole population. In other words, if we view the whole population as a single entity, the population's performance (reflected by population means) can be explained adequately by the environmental effect captured by the PTT measurements. When environmental factors (photoperiod, GDD, and PTT) within a window are searched, it is expected to have some levels of correlation given that these periods are sections of the growing season environment and if these environmental measurements are the major factors underlying the phenotype. However, only when PTT (not GDD or photoperiod) was used were we able to obtain a consistently high correlation overall a stretch of overlapping windows.

Genomic prediction. For tested genotypes in untested environments, we conducted leave-one-environment-out cross-validation. In each run, 6 environments were used for model building to predict the performance of all genotypes in the remaining 1 environment. For untested genotypes in tested environments, we conducted leave-half-RILs-out cross validation. In each run, 50% of the RILs were randomly sampled for model building and the remaining 50% RIL for validation. For untested genotypes in untested environments, we conducted the combination of leave-one-environment-out and leave-half-RILs-out cross validation. In each run, performance data from the 50% of RILs across 6 environments were used for model building and performance data from the remaining 50% RILs in the remaining 1 environment were used for validation.

www.pnas.org/cgi/doi/10.1073/pnas.1718326115

Preliminary analysis of genomic prediction was carried out with several methods including ridge regression BLUP, BayesA BayesB, BayesC, BayesCπ, BayesRR, BayesLASSO, Gaussian kernel, and exponential kernel (2, 3). Ridge regression BLUP was chosen for further analyses because similar prediction accuracy values were obtained from different methods and because this approach was computationally less demanding.

The high overall prediction accuracy observed for all three scenarios is a combination of agreement between observed values and predicted values at individual environment and agreement between observed population mean value and predicted population mean value across environments.

Empirical validation. After the completion of the initial analysis and model building process, we decided to carry our empirical validation experiments. The mapping population was grown again in Ames IA summer nursery in 2015 and 2016 (IA15 and IA16) (table S1). Notably, the fluctuating temperature in early growing season at this location generated two different photothermal values. While IA16 was similar to IA13, IA15 was different from all other environments. Predicted flowering time for IA15 and IA16 was obtained through two joint genomic regression analysis (JGRA) approaches and through the QTL-based approach.

All relevant genotype, phenotype, and environment data are included (dataset S1)

Partitioning G × E into heterogeneity of genotypic variance and lack of genetic correlation. Following the steps laid out in previous publications (4-6), we first conducted variance component analysis across all environments using a linear mixed model (table S2). Second, we did variance analysis in each environment using linear mixed model to obtain genetic variance in each environment (table S3). Third, we partitioned the G × E interaction into component due to heterogeneity of genotypic variance among environment V and component due to lack of genetic correlation among environments L using equations:

$V = \frac{\sum_j (\sigma_{gj} - \bar{\sigma}_g)^2}{n_e - 1}$, where n_e is the number of environments; and $L = \sigma_{ge}{}^2 - V$

The genetic correlation is $r_g = \frac{\sigma_g{}^2}{\sigma_g{}^2 + L}$. The line mean heritability is estimated as

$h^2 = \frac{\sigma_g{}^2}{\sigma_g{}^2 + \frac{\sigma_{ge}{}^2}{n_e} + \frac{\sigma_\varepsilon{}^2}{n_e n_r}}$, where n_r is the number of replication.

Of total G × E observed, 56% is due to heterogeneity of genotypic variance and 44% due to lack of genotypic correlation (table S4).

Photothermal time identified as an environmental index for a set of sorghum accessions. We retrieved the data from an earlier study where monthly planting of a set of 8 sorghum maturity testers ($Ma_1 – Ma_4$) were planted in 12 consecutive months in Mayaguez, Puerto Rico (Table 4 of the original publication) (7). The same analysis procedure was applied in pattern detection and window search to identify the environmental index by photothermal time.

Photothermal time correlation with mean flowering time for different experiment settings. The flowering time and environmental settings (photoperiod and temperature) in experiments in 40 species were retrieved from the literature where the study of photoperiod and temperature effects was explicitly stated in the title and abstract.

Species	Common name	References
Arabidopsis thaliana		(8)
Arachis hypogaea	Peanut	(9)
Avena sativa	Oat	(10)
Bouteloua gracilis	Blue grama	(11)
Brassica pekinesis	Chinese cabbage	(12)
Bromus tectorum	Downy brome	(13)
Cajanus cajan	Pigeonpea	(14)
Cicer arietinum	Chickpea	(15)
Crupina vulgaris	Common crupina	(16)
Dianthus carthusianorum		(17)
Fagopyrum esculentum	Buckwheat	(18)
Fragaria x ananassa	Strawberry	(19)
Glycine javanica		(20)
Helianthus annus	Sunflower	(21)
Heliotropium arborescens	Heliotrope	(22)
Hibiscus esculentus	Okra	(23)
Kochia scoparia	Kochia	(24)
Lens culinaris	Lentil	(25)
Liquidambar styraciflua	Sweetgum tree	(26)
Mucuna spp.	Velvet bean	(27)
Nicotiana tabacum	Tobacco	(28)
Parthenium hysterophorus		(29)
Pennisetum typhoides	Pearl millet	(30)
Persea americana	Avocado	(31)
Pisum sativum	Pea	(32)
Sesamum indicum	Sesame	(33)
Sorghum bicolor	Sorghum	(34)
Trifolium baccarinii		(35)
Trifolium masaiense		(35)
Trifolium pseudostriatum		(35)
Trifolium rueppellianum		(35)
Trifolium semipilosum		(35)
Trifolium steudneri		(35)
Trifolium tembense		(35)
Trifolium usambarense		(35)
Triticum aestivum	Wheat	(36)
Vigna radiata	Mungbean	(37)
Vigna subterranea	Bambara groundnut	(38)
Vigna unguiculata	Cowpea	(39)
Zea mays	Maize	(40)

References

1. Hammer GL*, et al.* (1989) Genotype-by-environment interaction in grain sorghum 2. Effects of temperature and photoperiod on ontogeny. *Crop Science* 29(2):376-384.
2. Meuwissen THE, Hayes BJ, & Goddard ME (2001) Prediction of total genetic value using genome-wide dense marker maps. *Genetics* 157(4):1819-1829.
3. Whittaker JC, Thompson R, & Denham MC (2000) Marker-assisted selection using ridge regression. *Genetical Research* 75(2):249-252.
4. Gibson G & van Helden S (1997) Is function of the *Drosophila* homeotic gene ultrabithorax canalized? *Genetics* 147(3):1155-1168.
5. Cooper M & Delacy IH (1994) Relationships among analytical methods used to study genotypic variation and genotype-by-environment interaction in plant breeding multi-environment experiments. *Theor Appl Genet* 88(5):561-572.
6. Yamada Y (1962) Genotype × environment interaction and genetic correlation of the same trait under different environments. *Janpanese Journal of Genetics* 37:498-509.
7. Miller FR, Barnes DK, & Cruzado HJ (1968) Effect of tropical photoperiods on growth of sorghum when grown in 12 monthly plantings. *Crop Science* 8(4):499-509.
8. Burghardt LT*, et al.* (2016) Fluctuating, warm temperatures decrease the effect of a key floral repressor on flowering time in *Arabidopsis thaliana*. *New Phytol* 210(2):564-576.
9. Bagnall DJ & King RW (1991) Response of peanut (*Arachis hypogaea*) to temperature, photoperiod and irradiance 1. Effect on flowering. *Field Crop Res* 26(3-4):263-277.
10. Bleken MA & Skjelvag AO (1986) The phenological development of Oat (*Avena Sativa* L.) cultivars as affected by temperature and photoperiod. *Acta Agr Scand* 36(4):353-365.
11. Benedict HM (1940) Effect of day length and temperature on the flowering and growth of four species of grasses. *J Agric Res* 61:0661-0671.
12. Moe R & Guttormsen G (1985) Effect of photoperiod and temperature on bolting in Chinese cabbage. *Sci Hortic-Amsterdam* 27(1-2):49-54.
13. Richardson JM, Morrow LA, & Gealy DR (1986) Floral induction of downy brome (*Bromus tectorum*) as influenced by temperature and photoperiod. *Weed Sci* 34(5):698-703.
14. Turnbull L, Whiteman P, & Byth D (1980) The influence of temperature and photoperiod on floral development of early flowering pigeonpea. *Proceedings of the International Workshop on Pigeonpeas*, pp 217-222.
15. Daba K, Tar'an B, Bueckert R, & Warkentin TD (2016) Effect of temperature and photoperiod on time to flowering in Chickpea. *Crop Sci* 56(1):200-208.
16. Patterson DT & Mortensen DA (1985) Effects of temperature and photoperiod on common crupina (*Crupina vulgaris*). *Weed Sci* 33(3):333-339.
17. Moe R (1983) Temperature and daylength responses in *Dianthus carthusianorum* cv. Napoleon III. *II International Symposium on Carnation Culture 141*, pp 165-172.
18. Lachmann S & Adachi T (1990) Studies on theinfluence of photoperiod and temperature on floral traits in Buckwheat (*Fagopyrum Esculentum* Moench) under controlled stress conditions. *Plant Breeding* 105(3):248-253.
19. Sønsteby A & Heide O (2007) Quantitative long-day flowering response in the perpetual-flowering F1 strawberry cultivar Elan. *The Journal of Horticultural Science and Biotechnology* 82(2):266-274.
20. Wutoh J, Hutton E, & Pritchard A (1968) The effects of photoperiod and temperature on flowering in *Glycine javanica*. *Australian Journal of Experimental Agriculture* 8(34):544-547.
21. Robinson RG (1971) Sunflower phenology - year, variety, and date of planting effects on day and growing degree-day summations. *Crop Sci* 11(5):635-638.

22. Park BH & Pearson S (2000) Environmental regulation of flowering time in heliotrope (*Heliotropium arborescens* L. cv. Marine). *Sci Hortic-Amsterdam* 85(3):231-241.
23. Tenga AZ & Ormrod DP (1985) Responses of Okra (*Hibiscus Esculentus* L) cultivars to photoperiod and temperature. *Sci Hortic-Amsterdam* 27(3-4):177-187.
24. Bell AR, Nalewaja JD, & Schooler AB (1972) Light period, temperature, and Kochia flowering. *Weed Sci* 20(5):462-464.
25. Erskine W, Ellis RH, Summerfield RJ, Roberts EH, & Hussain A (1990) Characterization of responses to temperature and photoperiod for time to flowering in a world lentil collection. *Theor Appl Genet* 80(2):193-199.
26. Williams GJ (1971) Phenology of 6 United-States Provenances of *Liquidambar styraciflua* under controlled conditions. *Am J Bot* 58(1):24-31.
27. Qi AM*, et al.* (1999) Differences in the effects of temperature and photoperiod on progress to flowering among diverse Mucuna spp. *J Agron Crop Sci* 182(4):249-258.
28. Seltmann H (1974) Effect of light periods and temperatures on plant form of *Nicotiana tabacum* L Cv Hicks. *Bot Gaz* 135(3):196-200.
29. Williams JD & Groves RH (1980) The influence of temperature and photoperiod on growth and development of *Parthenium hysterophorus* L. *Weed Res* 20(1):47-52.
30. Beeg JE & Burton GW (1971) Comparative study of five genotypes of pearl millet under a range of photoperiods and temperatures. *Crop Sci* 11(6):803-805.
31. Buttrose MS & Alexander DM (1978) Promotion of floral initiation in 'Fuerte' Avocado by low temperature and short daylength. *Sci Hortic-Amsterdam* 8(3):213-217.
32. Berry GJ & Aitken Y (1979) Effect of photoperiod and temperature on flowering in pea (*Pisum sativum* L.). *Aust J Plant Physiol* 6(5-6):573-587.
33. Suddihiyam P, Steer BT, & Turner DW (1992) The flowering of sesame (*Sesamum indicum* L) in response to temperature and photoperiod. *Aust J Agr Res* 43(5):1101-1116.
34. Quinby JR, Hesketh JD, & Voigt RL (1973) Influence of temperature and photoperiod on floral initiation and leaf number in sorghum. *Crop Sci* 13(2):243-246.
35. Mannetje LT & Pritchar.Aj (1968) Effects of photoperiod and night yemperature on flowering and growth in some African *Trifolium* species. *New Phytol* 67(2):257-263.
36. Slafer GA & Rawson HM (1995) Photoperiod X temperature interactions in contrasting wheat genotypes: Time to heading and final leaf number. *Field Crop Res* 44(2-3):73-83.
37. Aggarwal VD & Poehlman JM (1977) Effects of photoperiod and temperature on flowering in mungbean (*Vigna radiata* (L)Wilczek). *Euphytica* 26(1):207-219.
38. Linnemann AR & Craufurd P (1994) Effects of temperature and photoperiod on phenological development in three genotypes of bambara groundnut (*Vigna subterranea*). *Ann Bot-London* 74(6):675-681.
39. Ehlers JD & Hall AE (1996) Genotypic classification of cowpea based on responses to heat and photoperiod. *Crop Sci* 36(3):673-679.
40. Warrington IJ & Kanemasu ET (1983) Corn growth response to temperature and photoperiod .1. seedling emergence, tassel initiation, and anthesis. *Agron J* 75(5):749-754.

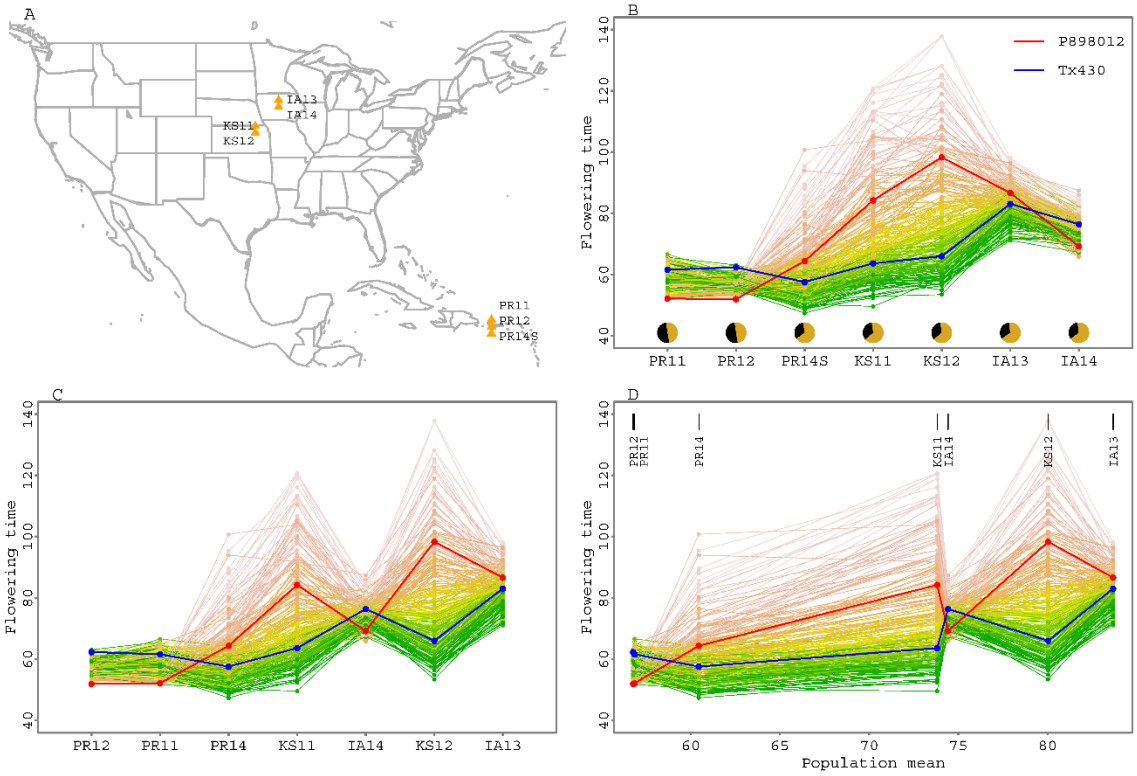

Figure S1. Flowering time expressed as days after planting is not a desirable choice to conduct the combined analysis and modeling. (**A**) Seven natural field environments; (**B**) Reaction norm based on a categorical order of photoperiod of testing sites; (**C**) Reaction norm based on a categorical order of population means for individual environments; (**D**) Reaction norm based on a numerical order of population means for individual environments.

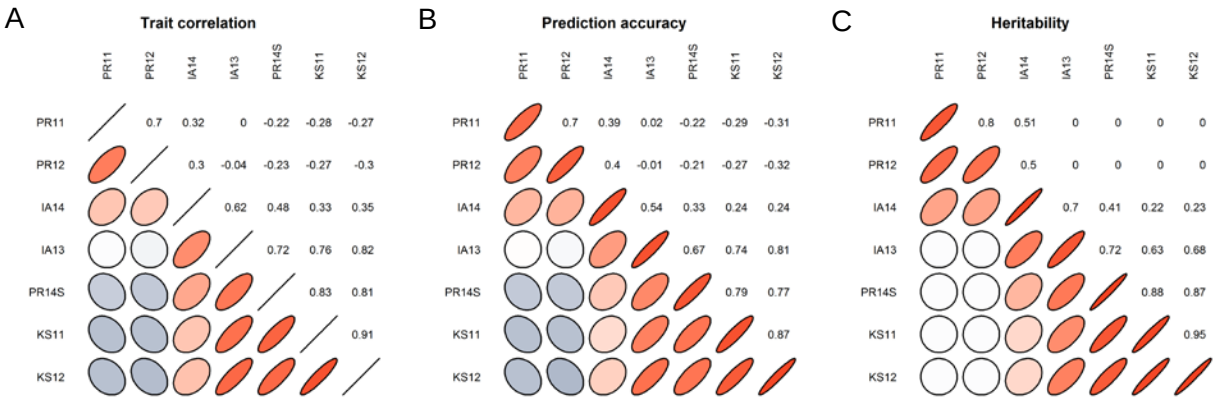

Figure S2. G × E in flowering time expressed as growing degree days (GDD) shows different trait correlations between environments. (**A**) Pair-wise trait correlations. (**B**) Prediction accuracy within individual environments (diagonal) and between environments (off diagonal and row to column). (**C**) Heritability within individual environments (diagonal) and between environments (when the analysis is done for the pair of environments together).

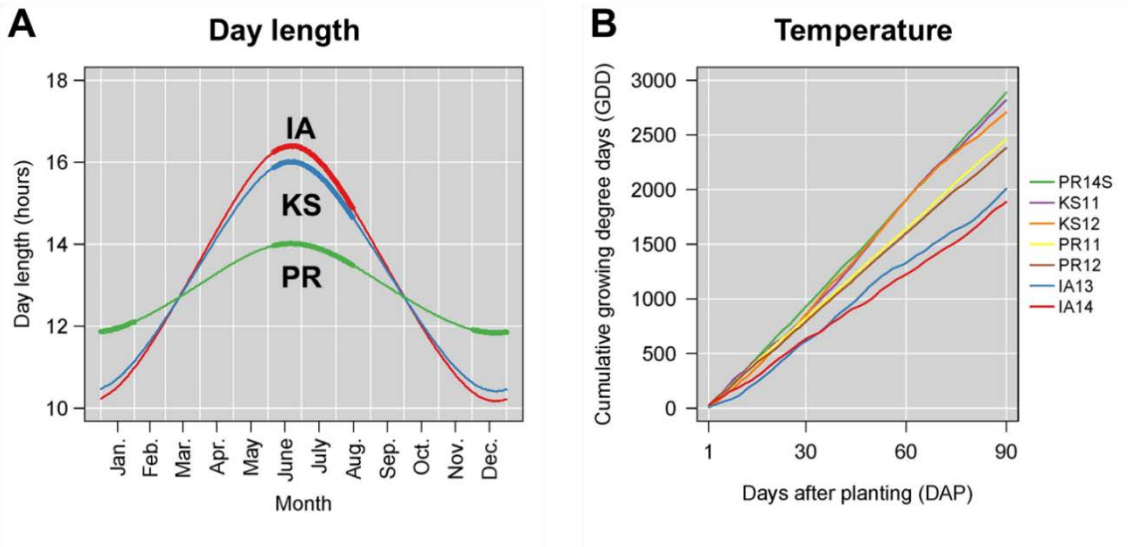

Figure S3. Day length and temperature profiles of seven environments. (**A**) Day length. The bold segments of the lines represent the time between planting and when most plants flowered. (**B**) Temperature profile spanning the time between planting and 90 days after planting.

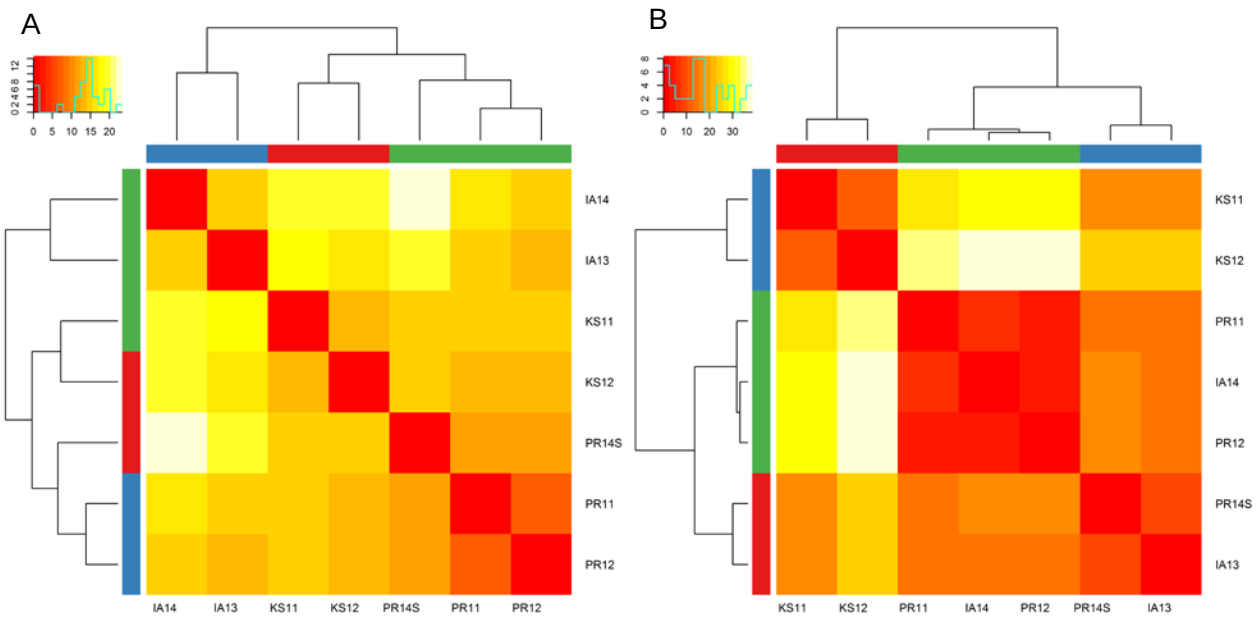

Figure S4. Clustering of seven environments. (**A**) Clustering based on temperature profile during grown seasons. (**B**) Clustering based on flowering time of the RIL population.

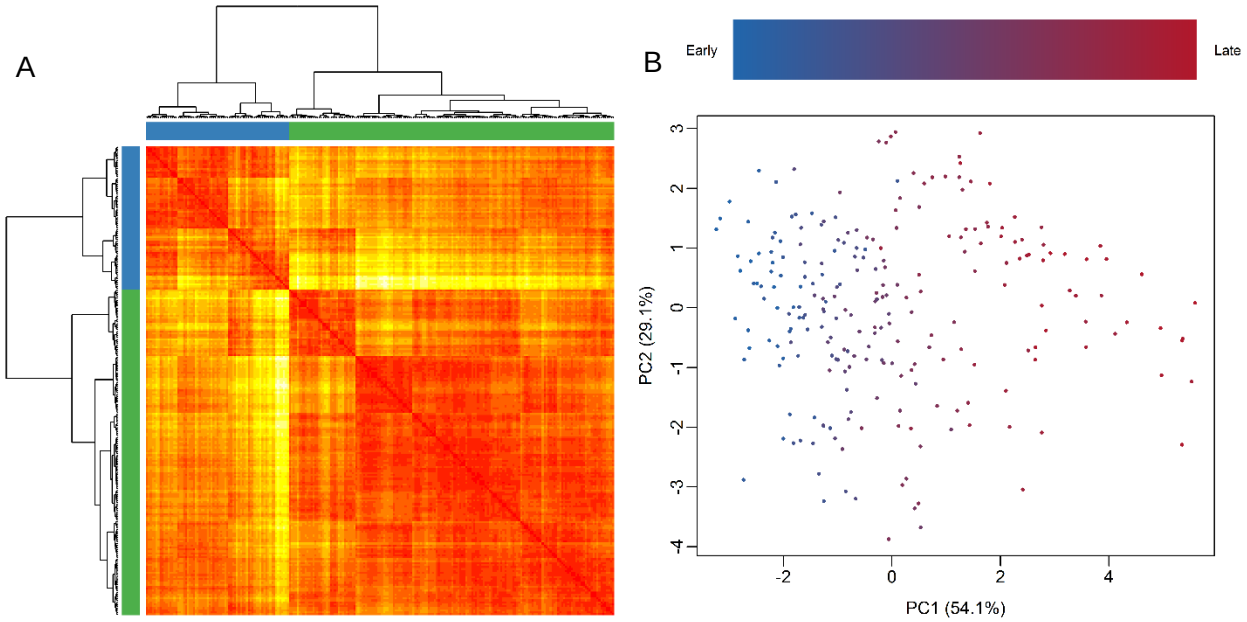

Figure S5. Clustering of the RILs based on their flowering time value observed across seven environments. (**A**) Hierarchical clustering of the RILs indicated one group with relatively stable flowering time (green bar) and the second group with varied flowering time (blue bar). (**B**) Principal component analysis indicated that RILs with high plasticity flower late in Kansas environments.

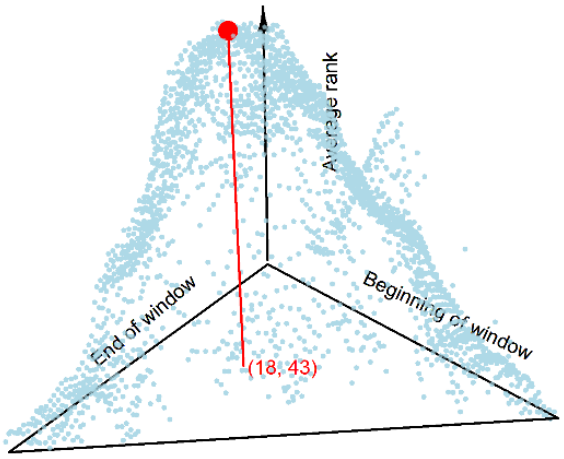

Figure S6. Subsampling analysis to search for the windows within which the photothermal time is highly correlated with the population means observed in different environments. Leave-one-environment-out analysis was conducted. In Figure 2B, the (18, 43) window is well supported by other surrounding windows, which agrees with the results of subsampling analysis. On the other hand, other windows, for example (26, 27), are not supported by the subsampling analysis.

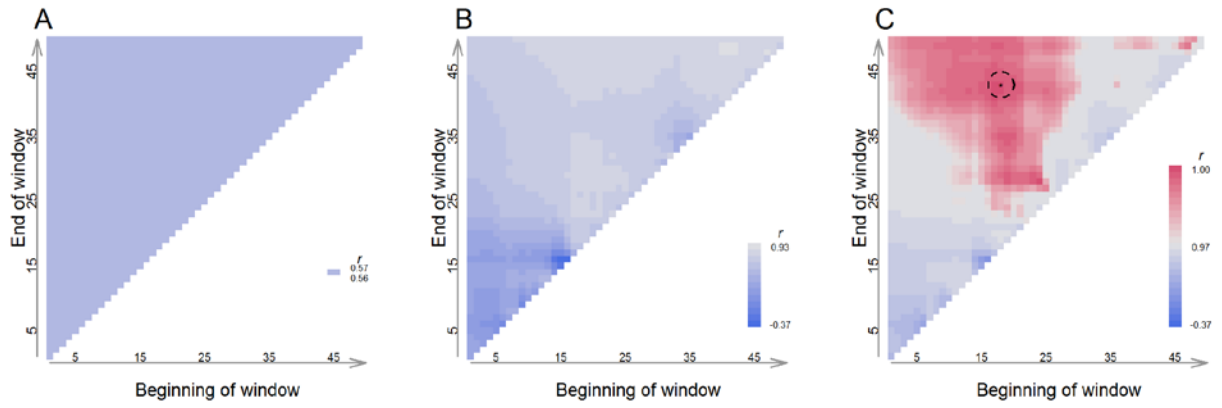

Figure S7. Correlation between population mean and each of the three environmental parameters across different windows. (**A**) Photoperiod. (**B**) Temperature (GDD). (**C**) Photothermal time. Because of the temporal patterns of environmental factors, it is expected that window search can identify a cluster of windows with similar correlation strength. The choice of the best window should be from a region of the matrix where high correlation values are found, rather than a small window with less support from the nearby region. In addition, subsampling analysis (Figure S6) and biological interpretation (Figure S8) should also be considered to avoid choosing windows that happen to show high correlation but with reduced predictive power and that is difficult to have reasonable biological interpretations.

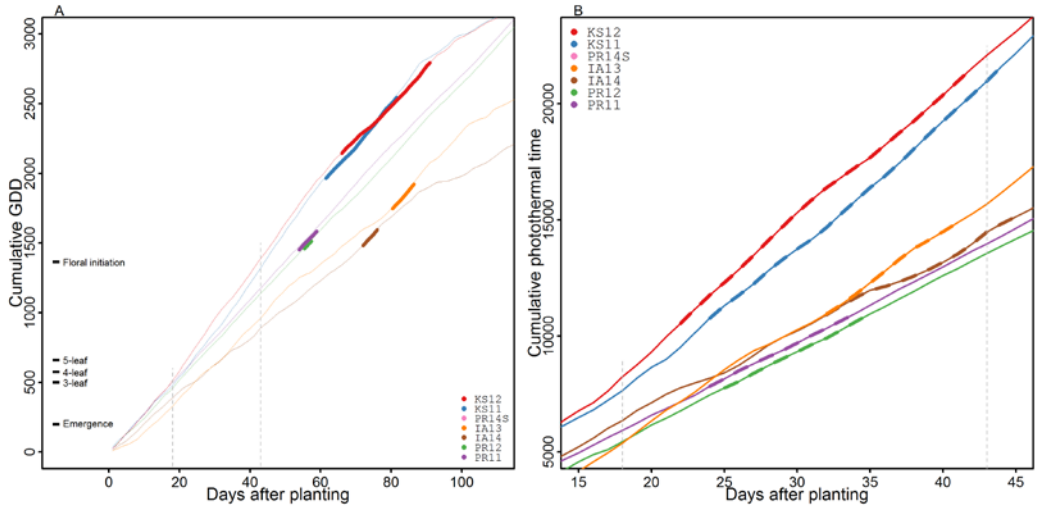

Figure S8. Projected growth stage where photoperiod and temperature sensing and vegetative-to-reproductive transition at individual environments. (**A**) Cumulative GDD, a general growth stage indicator, was plotted against days after planting. Two dashed lines define the critical 18~43 day-after-planting window. Bold segment corresponds to the inter quantile range within which 50% of the RILs flowered. (**B**) Cumulative photothermal time was plotted against days after planting. Two dashed lines define the critical 18~43 day-after-planting window. The projected critical stage, 3-leaf to floral initiation, was indicted with bold segments.

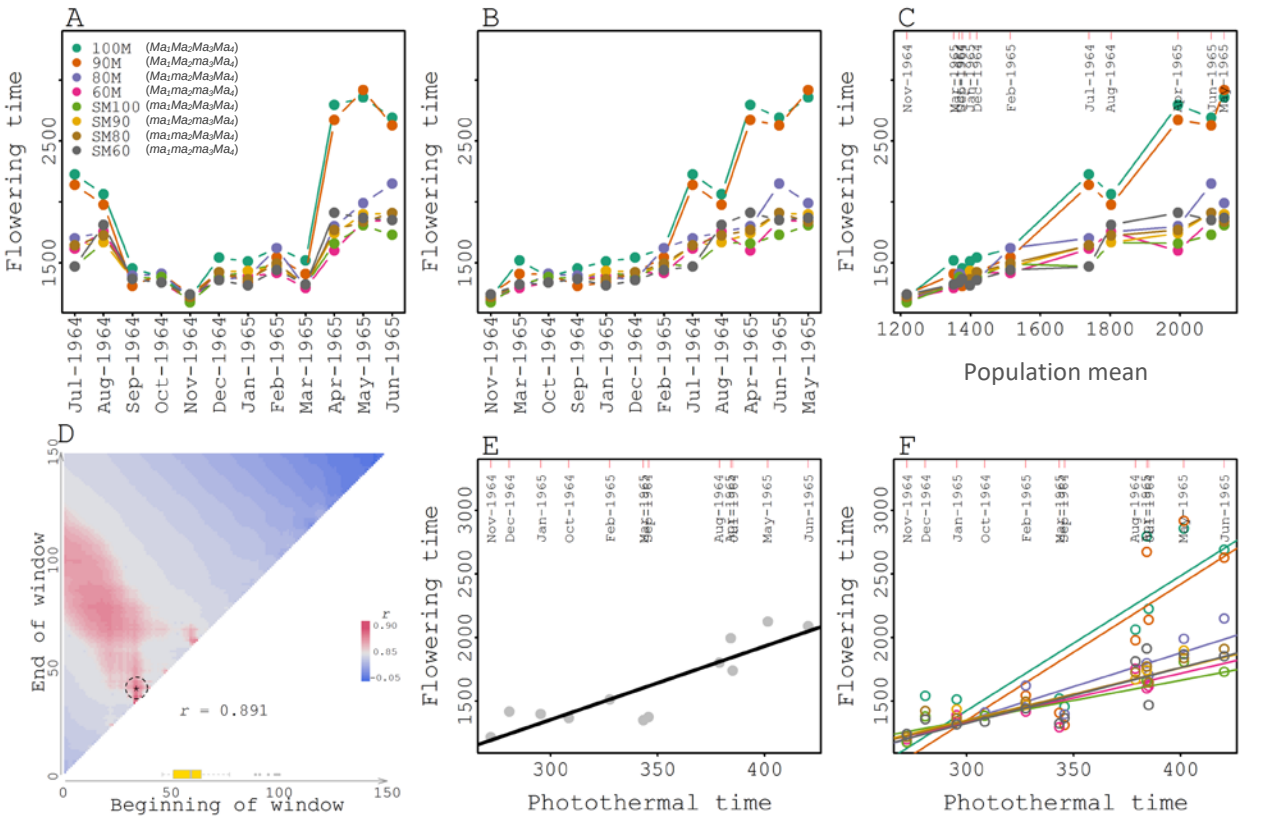

Figure S9. Pattern finding in flowering time G × E of a set of diverse sorghum accessions planted monthly. Progression from data visualization to pattern discovery: (**A**) Reaction norm based on chronological order of the planting month. (**B**) Reaction norm based on a categorical order of population means for individual environments. (**C**) Reaction norm based on a numerical order of population means for individual environments. (**D**) Exhaustive search of the photothermal time window. (**E**) Correlation between population mean and photothermal time of the selected window. (**F**) Reaction norms based on the photothermal-time gradient. Actual observations shown with circles and regression fitted values shown with the lines. *Ma*$_1$ – *Ma*$_4$ are four maturity loci defined in classical sorghum genetics literature. Two genotypes homozygous dominant for both *Ma*$_1$ and *Ma*$_2$ (*i.e.*, 100M and 90M) have higher phenotypic plasticity than other genotypes.

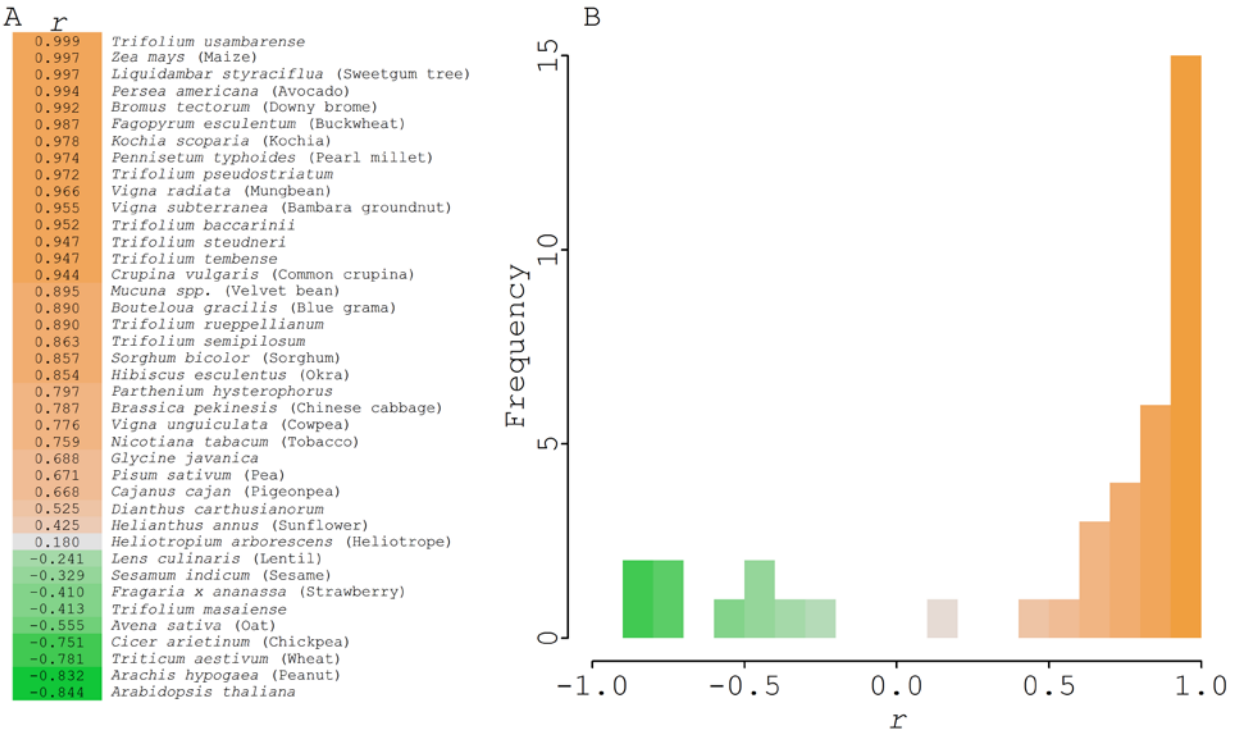

Figure S10. Correlation between photothermal time and flowering time among 40 experiments (|*r*| > 0.75 for 29 experiments) where flowering time was studied under different combinations of photoperiod and temperature settings. (**A**) Correlation for studies in different species. (**B**) Frequency distribution for correlation coefficient. Please see SI Materials and Methods for the original publications of these 40 experiments. In each experiment, photothermal time is calculated from the stated photoperiod and temperature setting values, and average flowering time (expressed as growing degree days) of all genetic material under each combination of photoperiod and temperature setting is obtained. Correlation between these photothermal time values and the average flowering time is calculated across all settings for each experiment.

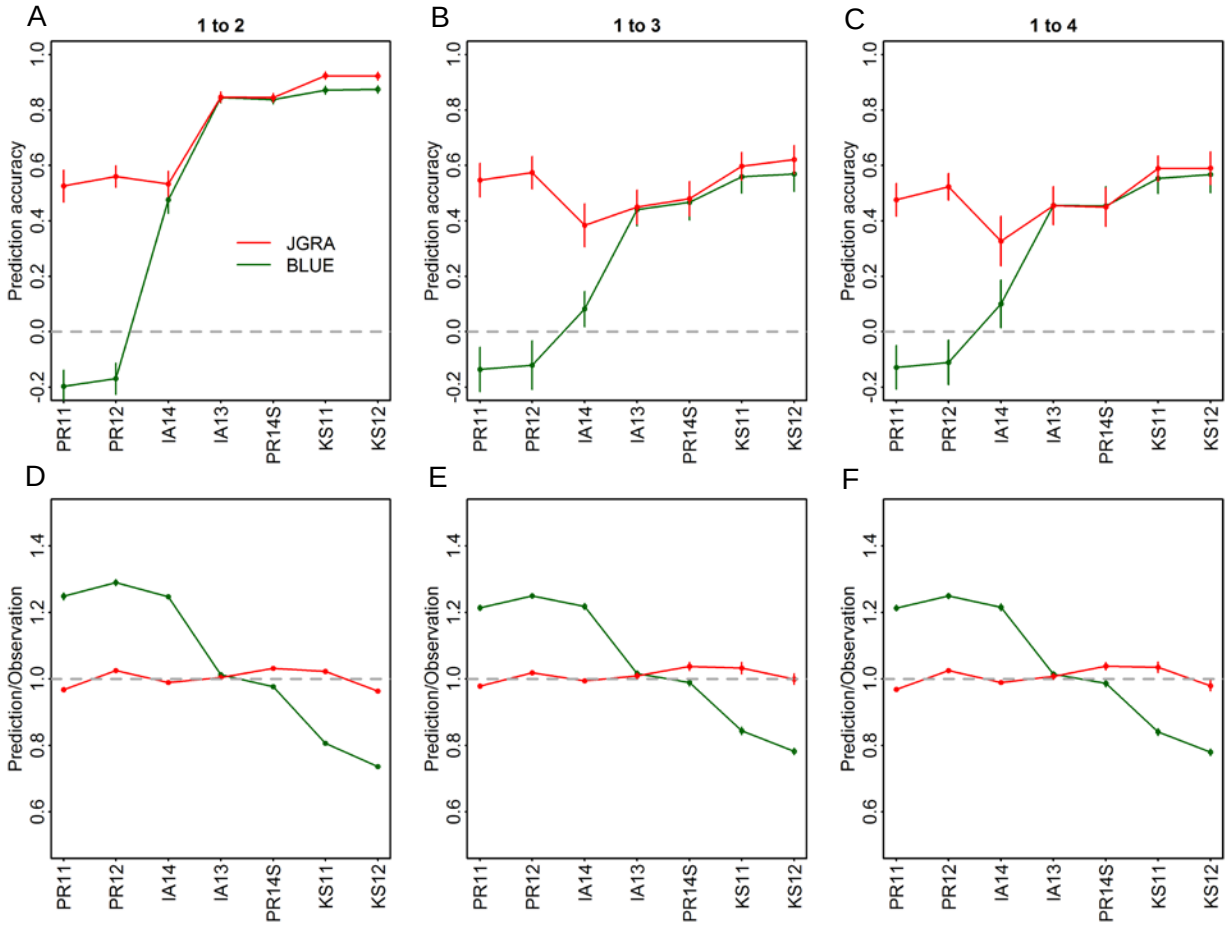

Figure S11. Prediction accuracy of joint genomic regression analysis (JGRA) through reaction-norm parameters compared with predictions relying on averages across tested environments (BLUE, best linear unbiased estimation). Performance prediction for tested genotype under untested environment (1 to 2), for untested genotype under tested environment (1 to 3), and for untested genotype under untested environment (1 to 4). Prediction accuracy for: 1 to 2 (**A**); 1 to 3 (**B**); and 1 to 4 (**C**). Average ratio of predicted versus observed values for: 1 to 2 (**D**); 1 to 3 (**E**); and 1 to 4 (**F**).

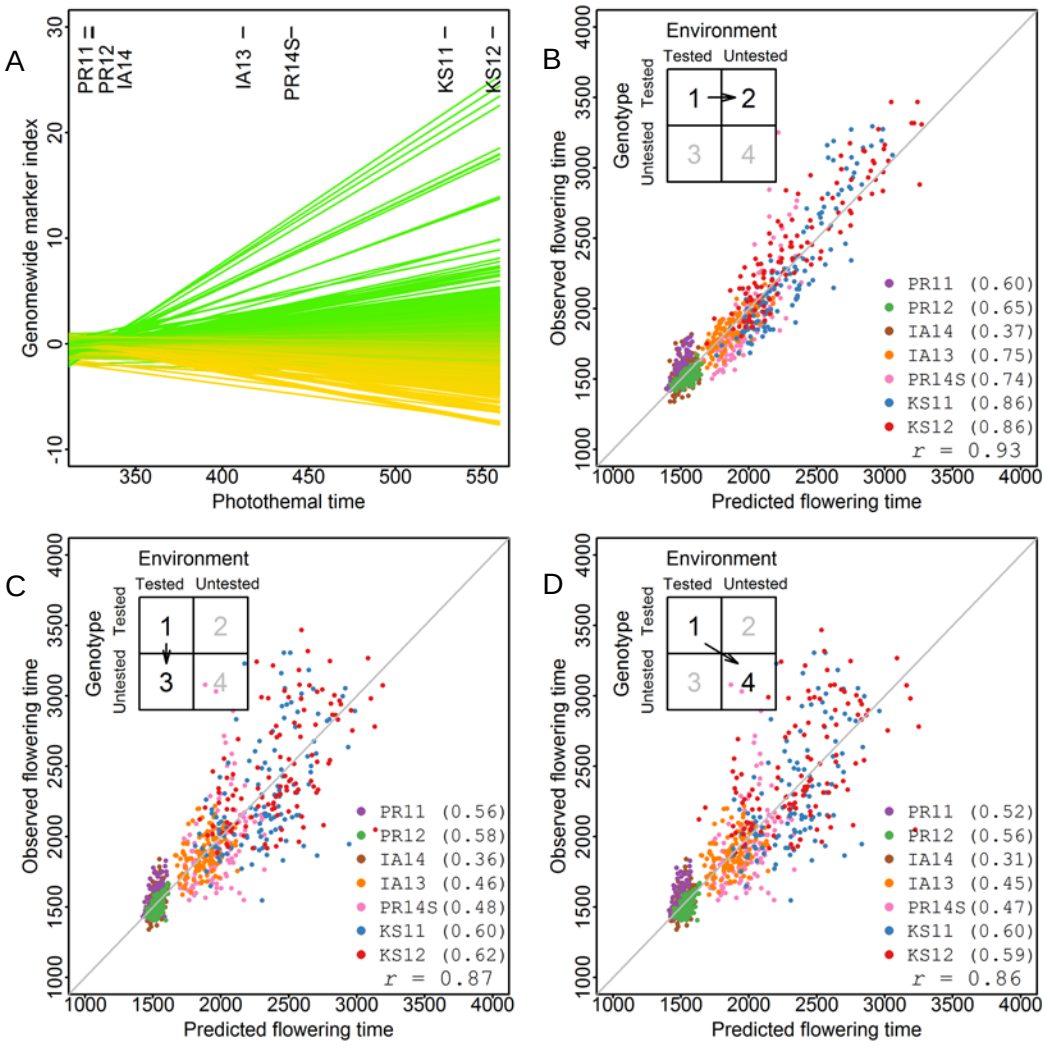

Figure S12. Joint genomic regression analysis for performance prediction with genome-wide marker effect continua. (**A**) Fitted genome-wide marker effects along the environmental index. (**B**) Predicting tested genotypes in untested environments. (**C**) Predicting untested genotypes in tested environments. (**D**) Predicting untested genotypes in untested environments. Both prediction accuracy at each individual environment (in parentheses) and across all environments (*r*) are shown. Diagonal line in B-D indicates the ratio of observed over predicted value being one. Average prediction accuracy for individual environments is 0.69, 0.52, and 0.50 for B, C, and D, respectively.

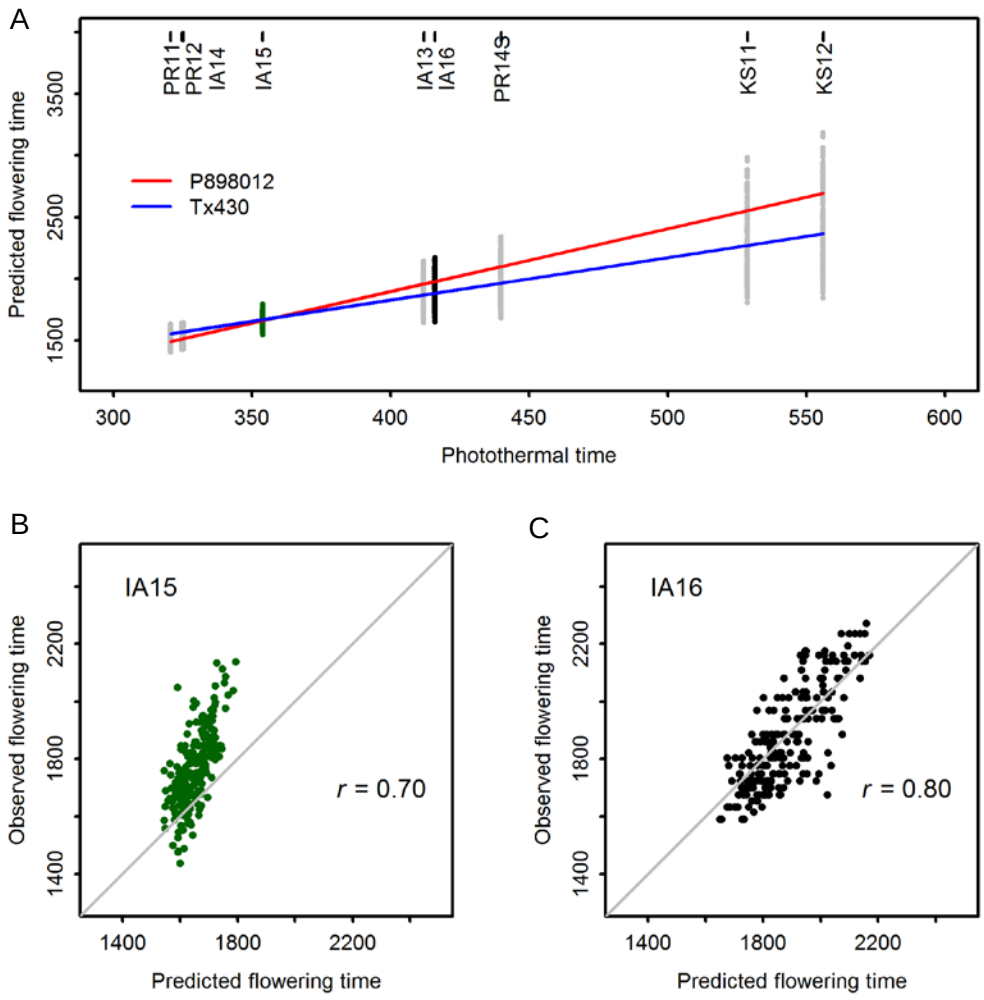

Figure S13. Empirical validation of performance prediction of JGRA with genome-wide marker effect continua. (**A**) Predicted flowering time of genotypes across environments. (**B**) Prediction accuracy for Iowa 2015 (IA15). (**C**) Prediction accuracy for Iowa 2016 (IA16). Diagonal line in B-C indicates the exact match between observed and predicted values.

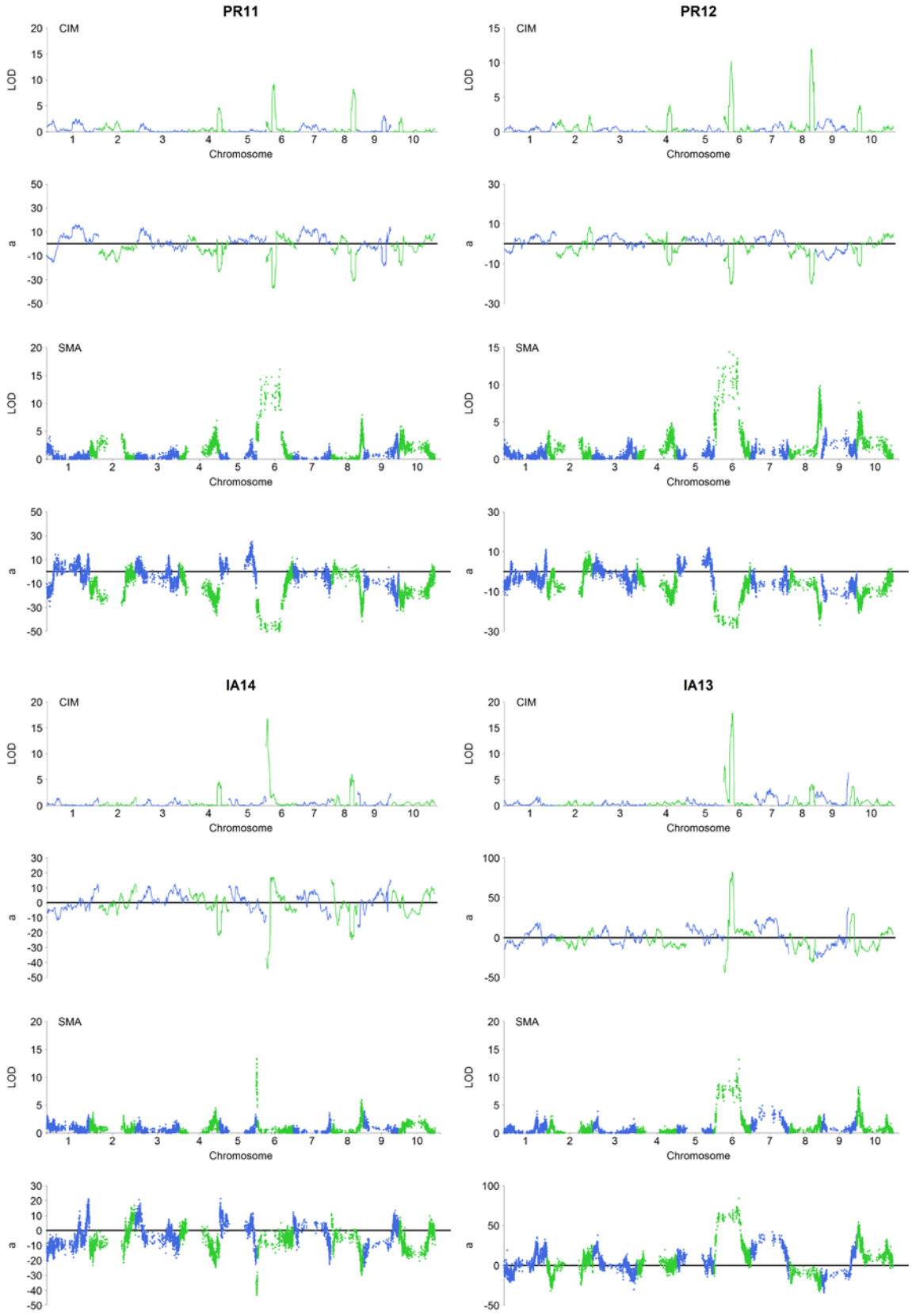
PR11
CIM
LOD
Chromosome
a
SMA
PR12
IA14
IA13

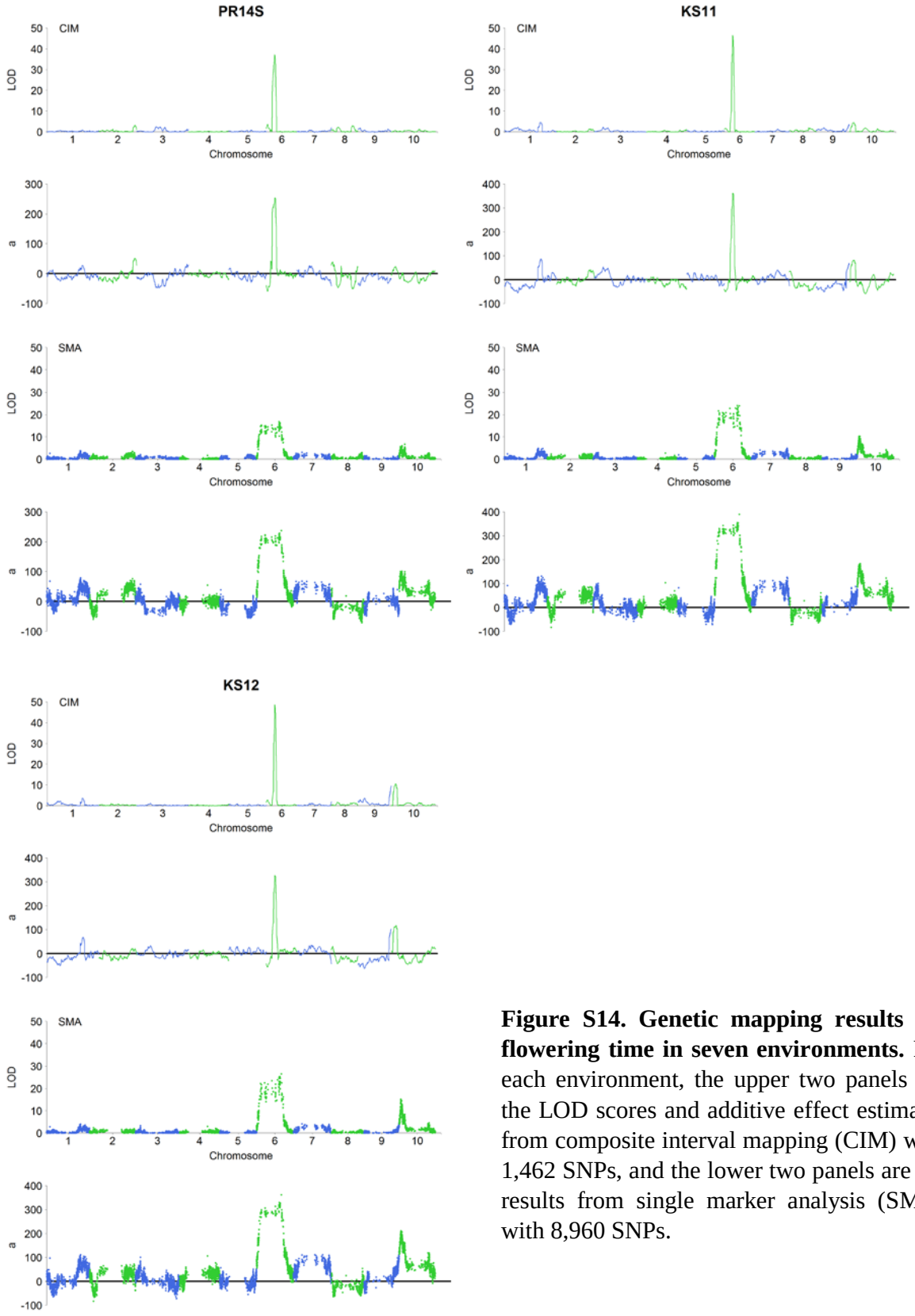

Figure S14. Genetic mapping results for flowering time in seven environments. For each environment, the upper two panels are the LOD scores and additive effect estimates from composite interval mapping (CIM) with 1,462 SNPs, and the lower two panels are the results from single marker analysis (SMA) with 8,960 SNPs.

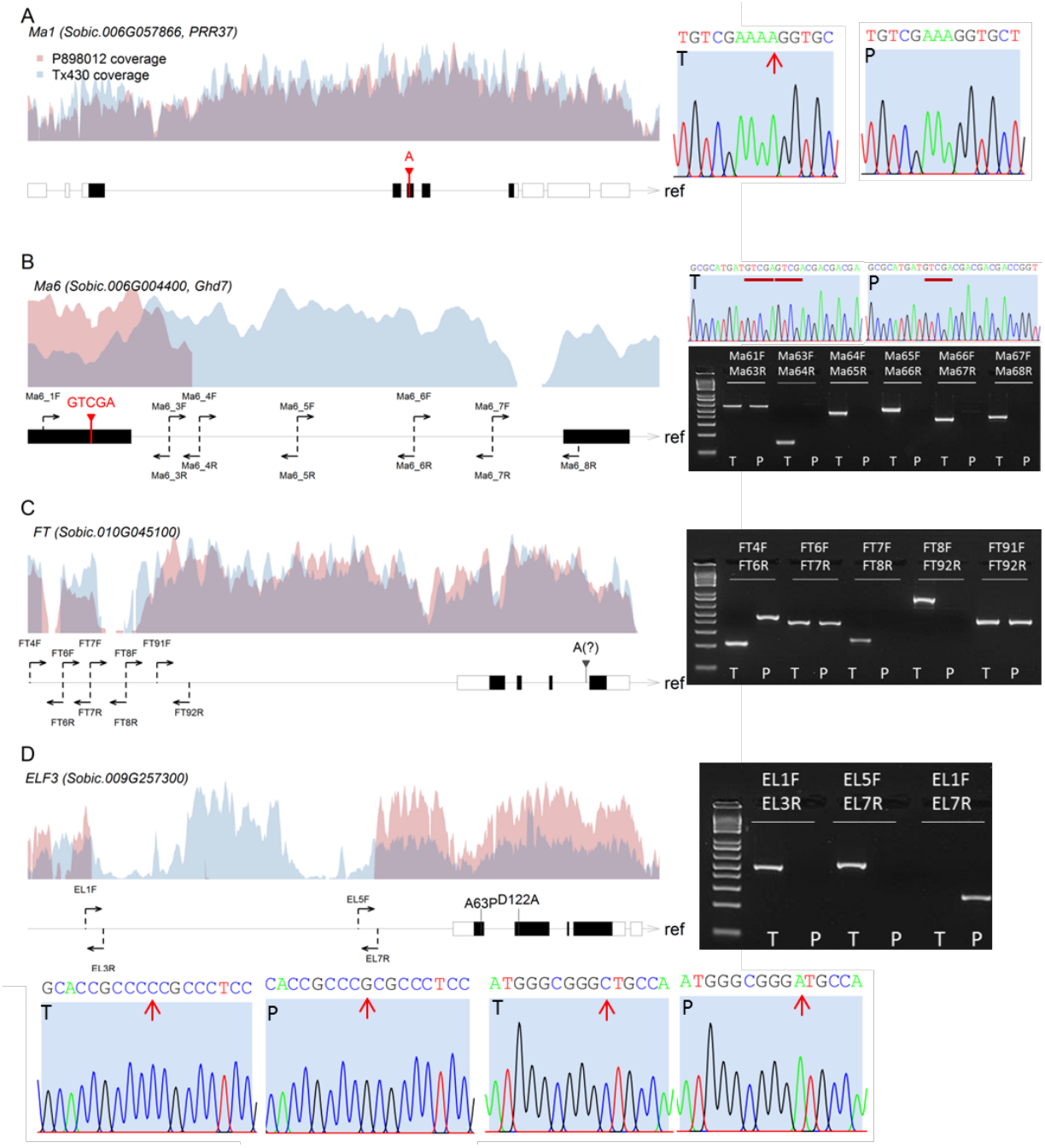

Figure S15. Detailed information about functional polymorphisms in four known or potential flowering time genes. (**A**) *PRR37* (*Ma*$_1$) on chromosome 6. Tx430 (T) allele has a single adenine insertion in the third exon. (**B**) *Ghd7* (*Ma*$_6$) on chromosome 6. The P898012 (P) allele had a large intron insertion, leading to a potentially modified CCT domain and a weak allele (*ghd7-2*); Tx430 allele had a 5 bp (GTCGA) insertion in the first exon, leading to a premature stop codon and nonfunctional protein (*ghd7-1*). (**C**) *Flowering Locus T* (*FT*) on chromosome 10. Tx430 allele has multiple adenine insertions in the third intron. P898012 allele of the *FT* gene contained a PIF/Harbinger transposon in the promoter region, potentially altering the binding site of another regulator. (**D**) *ELF3* is the potential gene underlying the QTL on chromosome 9. A 7.4-kb insertion of two copies of Gypsy LTR was detected in the promoter region of Tx430 allele, but not in P898012. Shaded curves on-top of gene models indicate the relative short read coverage of Tx430 and P898012.

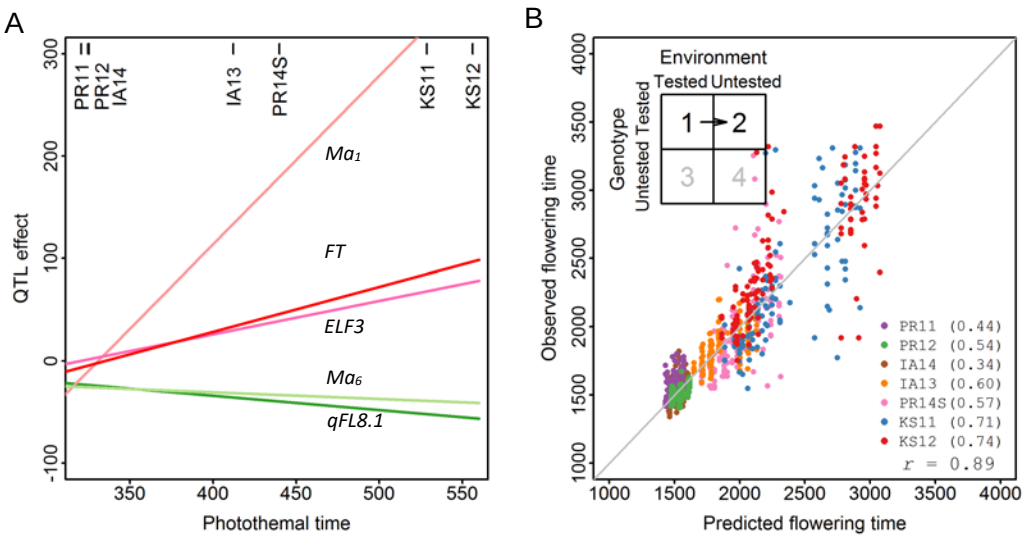

Figure S16. Joint genomic regression analysis for performance prediction with QTL effect continua. (**A**) Five fitted QTL effects along the photothermal-time environmental index. (**B**) Predicting tested genotypes in untested environments.

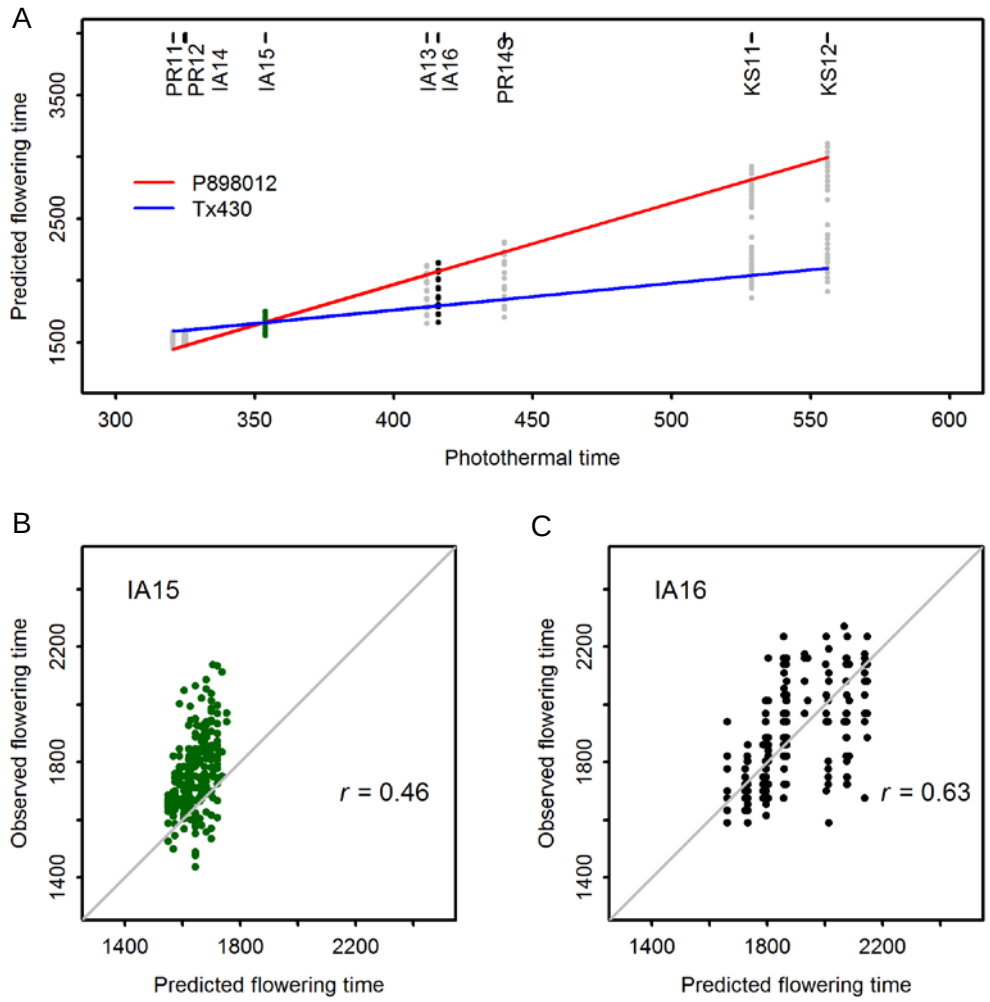

Figure S17. Empirical validation of performance prediction of JGRA with QTL effect continua. (**A**) Predicted flowering time of genotypes across environments. (**B**) Prediction accuracy for Iowa 2015 (IA15). (**C**) Prediction accuracy for Iowa 2016 (IA16). Diagonal line in B-C indicates the exact match between observed and predicted values.

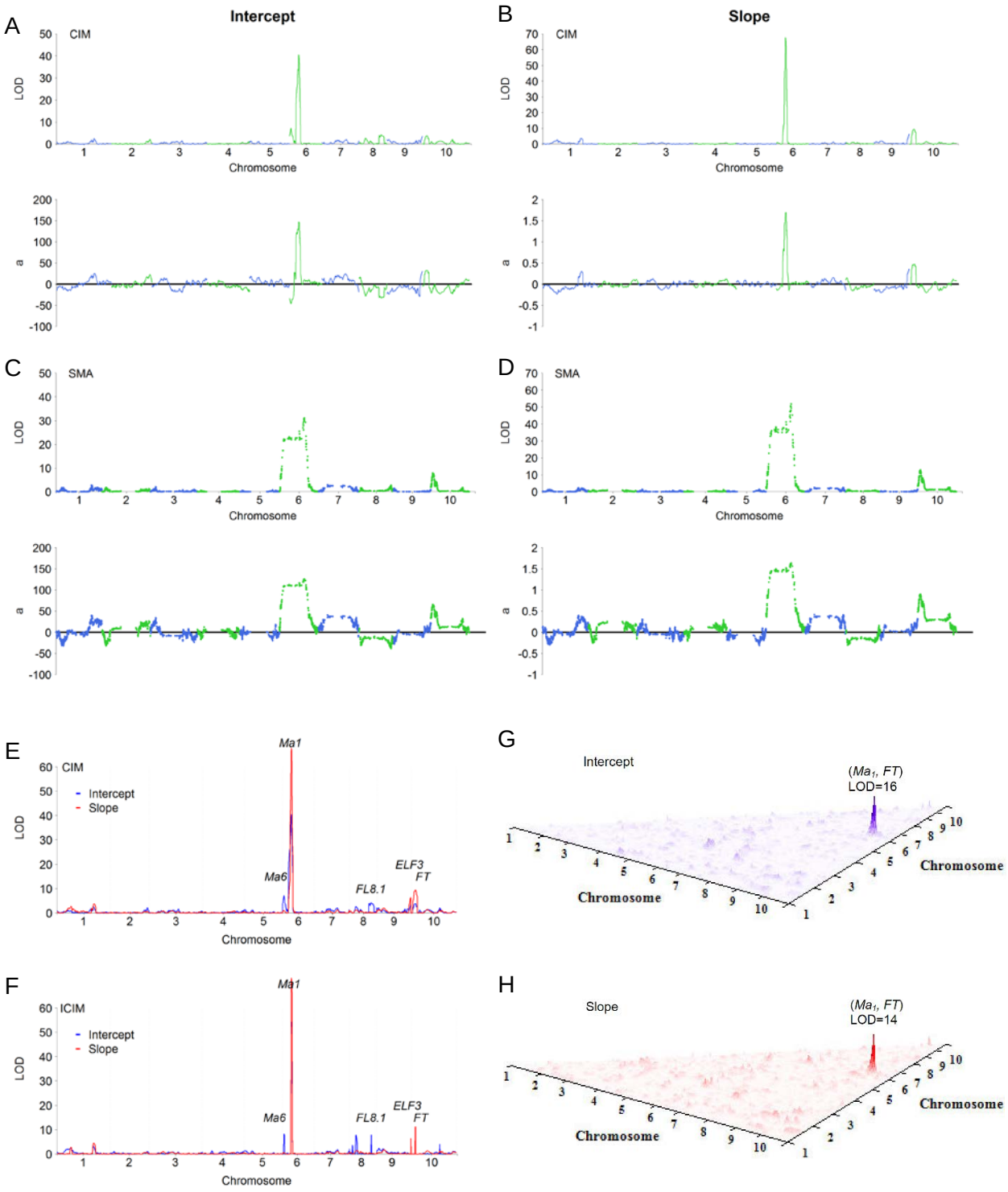

Figure S18. Genetic mapping results for reaction-norm parameters (intercept and slope). (**A-B**) LOD scores and additive effect estimates from composite interval mapping (CIM) with 1,462 SNPs. (**C-D**) Results from single marker analysis (SMA) with 8,960 SNPs. (**E-F**) Combined results from CIM and inclusive composite interval mapping (ICIM). (**G-H**) Epistasis search results for intercept and slope.

Table S1. Planting date and heritability of flowering time in each of the seven environments.

Environment	PR11*	PR12	PR14S	KS11	KS12	IA13	IA14	IA15	IA16
Nursery	Winter	Winter	Summer	Summer	Summer	Summer	Summer	Summer	Summer
Planting date	12/4/2010	12/12/2011	6/5/2014	6/8/2011	6/7/2012	6/3/2013	6/10/2014	6/10/2015	5/23/2016
Heritability	0.88	0.77	0.97	0.95	0.97	0.90	0.96	0.92	0.94

* Naming for the majority period of the nursery.

Table S2. Estimates of variance components from the combined analysis of seven environments.

Variance Component	**Estimate**	**Standard Error**	**Z Value**	**Pr > Z**	**Percent of Total**
Environment	141287.00	82895.00	1.70	0.04	62.99
Replication	4136.17	2217.86	1.86	0.03	1.84
Genotype	25788.00	3040.67	8.48	<1E-16	11.50
G × E	45951.00	1872.55	24.54	<1E-16	20.49
Residual	7150.59	252.59	28.31	<1E-16	3.19

Table S3. Estimates of genetic variances in each environment.

Environment	**Genetic variance (σ_g^2)**
PR11	10684.00
PR12	3386.46
IA14	8541.98
IA13	21107.00
PR14S	96668.00
KS11	188469.00
KS12	172502.00

Table S4. Estimates of variance components and parameters for the combined analysis of flowering time tested in seven environments.

Variance components and parameters	Estimate	Ratio to G × E
Genotype (σ_g^2)	25788.00	0.56
G × E interaction (σ_{ge}^2)	45951.00	-
Heterogeneity of genotypic variance	25643.58 (56%)	-
Lack of genetic correlation	20307.42 (44%)	-
Error (σ_ε^2)	7150.59	0.16
Line mean heritability (h^2)	0.78	-
Pooled genetic correlation (r_g)	0.56	-

Table S5. Environmental mean, average G × E, photothermal time, temperature, and photoperiod in each environment.

Environment	Environmental mean	Average G × E	Photothermal time	Temperature	Photoperiod
PR11	1556.63	-0.43	320.71	27.0	11.9
PR12	1507.46	-0.50	324.76	27.2	11.9
IA14	1550.80	-0.44	325.3	20.1	16.2
IA13	1859.12	-0.06	412.04	25.3	16.3
PR14S	1937.39	0.08	439.95	31.5	14.0
KS11	2289.25	0.56	528.72	33.4	15.8
KS12	2459.63	0.79	556.16	35.1	15.8

Note: To investigate the relationship between G × E and environmental parameters, we first obtained the G × E effect estimates for each RIL in individual environments. We considered average G × E effect of 237 RILs as a response variable (y), and considered photothermal time, temperature, and photoperiod as independent variables (x), to build the linear functions. With this approach, we found that photothermal time, temperature, and photoperiod, explained 99.1%, 70.4%, and 29.3% of the total variation in average G × E effect, respectively. With environmental mean (*i.e.*, population mean at an individual environment) as a response variable (y), we found that photothermal time, temperature, and photoperiod, explained 99.3%, 69.4%, and 30.5% of the total variation in environmental mean, respectively.

Table S6. The R^2 for the regression of phenotype on the predicted values at seven environments.

Environment	R^2
PR11	0.63
PR12	0.49
IA14	0.60
IA13	0.78
PR14S	0.81
KS11	0.94
KS12	0.95

Table S7. QTL detected for flowering time in seven environments using composite interval mapping. For each QTL, the first number is additive effect in GDD unit, the second number is support interval of additive effect, and the third number is phenotypic variance explained. Support interval of additive effect is estimated by using the average of two effects from 1 LOD drop from the peak.

Environment	**Chr1: 175.39 cM (~58 Mb)**	**Chr4: 153.73 cM (~ 61 Mb)**	**Chr6: 4.27 cM (~0.7 Mb)**	**Chr6: 40.92 cM (~42 Mb)**	**Chr7: 77.69 cM (~15 Mb)**	**Chr8: 111.38 cM (~53Mb)**	**Chr9: 163.91 cM (~59 Mb)**	**Chr10: 22.69 cM (~3 Mb)**
	-	-	*Ma*$_6$	*Ma*$_1$	-	*qFL8.1*	*ELF3*	*FT*
PR11		-23.19		-37.14		-31.21	-18.94	-18.59
		1.33		0.43		0.94	1.73	1.99
		5.44%		11.47%		10.10%	3.73%	3.24%
PR12		-11.09		-20.47		-20.05		-11.13
		0.78		0.74		0.79		1.04
		4.39%		12.07%		14.37%		4.19%
IA14		-22.14	-43.78			-24.88		
		1.34	0.34			0.98		
		5.54%	22.51%			7.32%		
IA13			-43.88	82.46	25.8	-30.94	37.96	29.78
			1.70	1.40	2.81	2.35	1.56	1.33
			9.03%	25.85%	3.47%	5.11%	7.45%	4.23%
PR14S				249.52				
				10.18				
				50.83%				
KS11	85.92			359.88			69.6	80.21
	9.56			2.46			5.39	3.47
	4.04%			54.00%			2.65%	3.16%
KS12				326.07			102.64	117.05
				1.24			2.13	4.12
				46.60%			6.15%	7.15%

Table S8. Patterns of QTL additive effects for flowering time show G × E interaction can fall into four main categories: antagonistic pleiotropy (AP), conditional neutrality (CN), differential sensitivity (DS), and no G × E. The number is the percentage of each category out of all pair-wise environment combinations.

Environment	**Chr1: 175.39 cM (~58 Mb)**	**Chr4: 153.73 cM (~ 61 Mb)**	**Chr6: 4.27 cM (~0.7 Mb)**	**Chr6: 40.92 cM (~42 Mb)**	**Chr7: 77.69 cM (~15 Mb)**	**Chr8: 111.38 cM (~53Mb)**	**Chr9: 163.91 cM (~59 Mb)**	**Chr10: 22.69 cM (~3 Mb)**
	-	-	*Ma_6*	*Ma_1*	-	*qFL8.1*	*ELF3*	*FT*
AP	0	0	0	38.10%	0	0	14.29%	28.57%
CN	28.57%	57.14%	47.62%	28.57%	28.57%	57.14%	57.14%	47.62%
DS	0	9.52%	0	33.33%	0	23.81%	14.29%	19.05%
No G × E	71.43%	33.33%	52.38%	0	71.43%	19.05%	14.29%	4.76%